CLM-P774

CLM-P774

UKAEA

Preprint

CIRCULAR & NON-CIRCULAR NOZZLE EXITS FOR SUPERSONIC GAS JET ASSIST IN CO_2 LASER CUTTING

J. FIERET
B. A. WARD

CULHAM LABORATORY
Abingdon Oxfordshire
1986

CIRCULAR AND NON-CIRCULAR NOZZLE EXITS FOR SUPERSONIC GAS JET ASSIST IN CO_2 LASER CUTTING

J Fieret & BA Ward
Laser Applications Group
UKAEA Culham Laboratory
Abingdon, Oxon OX14 3DB, UK

ABSTRACT

CO_2 laser cutting equipment utilises a cut assisting gas jet from a nozzle directed at the workpiece. At nozzle pressures in excess of 89kPa (gauge) the flow in the jet becomes supersonic. Shock structures in the jet can cause large variations in effective gas pressure on the workpiece.

Pressure measurement techniques and cutting trials with a conventional circular exit nozzle have demonstrated a strong correlation between maximum cutting speed and effective gas pressure on the workpiece (for optimum values of other cutting constants). A high effective pressure on the workpiece can be reached at impractically small nozzle to workpiece distances. At a practical distance (3-4mm) the shock structure in the jet limits the maximum workpiece pressure with a circular 1.5mm diameter exit nozzle to 300kPa (gauge).

A wide variety of circular and non-circular exit nozzles has been investigated by optical flow visualisation and pressure measurement techniques. Some non-circular exit designs achieve a workpiece pressure well in excess of 600kPa (gauge). A qualitative supersonic jet impingement model is presented in which it is suggested that the formation of a Mach shock disc in the jet must be avoided for a high workpiece pressure at practical working distance. The design of suggested nozzle exits is given, together with the associated pressure distributions.

To be published in the proceedings of the 'Lasers in Manufacturing 3' Conference, Paris, France 3-5 June 1986.

JANUARY 1986

INTRODUCTION

In gas jet assisted laser cutting of metals the laser beam is focused onto the surface of the workpiece. A gas jet is used to remove the molten metal and debris from the cut. The gas can be inert if the workpiece is to be protected against oxidation or active for a higher cutting speed from an exothermal reaction with the metal.

The cutting gas jet is formed by either a coaxial nozzle concentric with the focusing optics or an off-axis nozzle directed at the interaction point. A coaxial nozzle must be big enough to pass the focused laser beam without it touching the nozzle.

Conventional use of lasers for cutting has proved to be economical and reliable. However, there are a number of more demanding applications where cut quality, penetration or cutting speed have been found to be unpredictable or lacking in reproducibility.

The observations described in this paper result from a programme of work aimed at identification of important parameters of the cutting process, together with estimation of their best values and of the tolerance of the process to their variation.

The efficiency and reproducibility of removal of molten metal and debris from a cut can be shown to be strongly correlated with the effective cutting gas jet pressure on the workpiece (the workpiece pressure). Many operators of laser cutting systems use nozzle pressures above 89kPa(g) where the gas jet becomes supersonic. Above this pressure shocks are formed in the jet, causing flow patterns and pressure distributions which are sensitive functions of pressure applied to the nozzle, nozzle exit shape and dimensions and nozzle to workpiece distance.

Measurement of the workpiece pressure from a circular exit nozzle as a function of nozzle pressure and nozzle to workpiece distance clearly shows the operating range of these factors for which the flow and pressure on the workpiece provide an effective removal of material. It is also possible to identify areas of low workpiece pressure and where the gas flow is not effective at material removal.

This paper describes an investigation into the gas flow (shock structures and pressure distributions) in cutting jets from a wide range of nozzles with non-circular exit. The aim is to identify non-circular exit designs that give a high workpiece pressure and effective material removal, together with large tolerances in nozzle pressure and workpiece distance.

SUPERSONIC JETS WITH SHOCKS

Workpiece Pressure

It can be shown that for isentropic (i.e. frictionless and adiabatic) gas flow the total pressure along a streamline is constant and equal to the sum of the static (or hydraulic) and dynamic pressure. The total pressure is often called the stagnation pressure since it is the static pressure of the gas if its velocity were isentropically reduced to zero.

The workpiece pressure (i.e. the effective cutting gas jet pressure) which will be measured in this experiment is the static pressure on the surface on which a jet impinges. In the theoretical limit without heat transfer or friction and the streamlines perpendicular to the surface, the gas velocity is

isentropically reduced to zero and the workpiece pressure is equal to the local stagnation pressure. For example, if the gas flow in the nozzle and the jet is approximately isentropic (as for a subsonic jet) then the workpiece pressure is equal to the static pressure in the compressed gas holder behind the nozzle (the gas velocity in the holder is zero).

Properties of Shocks

A shock is an irreversible process and therefore not isentropic. This implies that the stagnation pressure along a streamline is not constant across a shock and in fact always decreases. Across a shock the mass density, temperature and static pressure can be shown to increase. The strength of a shock is a function of the specific heat ratio and the upstream Mach number (i.e. ratio of gas velocity over local sound velocity) only (see, for example, Von Mises [5]).

A normal shock is a shock perpendicular to the gas flow direction and can only occur in a flow that is initially supersonic. The gas velocity across a normal shock always changes from supersonic to subsonic values.

An oblique shock is not normal to the flow, and only the velocity component normal to the oblique shock is changed. This causes the velocity direction to be changed towards the shock. The downstream velocity can be either subsonic or supersonic, depending on the strength of the shock and the angle between velocity and shock.

Nozzle Flow

The flow inside a converging nozzle can be shown to be always subsonic. The maximum velocity is reached in the narrowest section i.e. in the exit. This velocity will be sonic if

$$\frac{p_n}{p_a} \geq \left[\frac{2}{\gamma+1}\right]^{\frac{\gamma}{1-\gamma}} \qquad (1)$$

p_n is the nozzle (stagnation) pressure and p_a the ambient pressure. γ is the specific heat ratio. For air $\gamma=1.4$, and sonic velocity in the nozzle exit is reached for $p_n/p_a \geq 1.89$. Above this pressure the velocity remains sonic but the static pressure in the exit will rise to values above p_a. This causes the flow at the exit to expand suddenly to match the lower ambient pressure. The jet is now supersonic and an axi-symmetric, converging shock is formed at the exit. Further downstream this shock can intersect at the jet axis and reflect on the jet boundary several times (fig. 1a).

For high ratio Pn/Pa the converging shock becomes curved and too strong to allow regular intersection as described above. Instead a normal shock that is stronger than the incident oblique shock is formed. This shock is called the Mach shock disk (MSD). The flow downstream of the MSD is subsonic and is separated from the outer flow by a slipstream (fig. 1b). Across this slipstream gradients in velocity, density, temperature and stagnation pressure exist.

Other investigators (Donaldson[1], Gubanova[2], Ginzburg[3], Kalghatgi[4]) have investigated the flow in supersonic impinging jets from circular orifices. They found that a vortex ring can exist on the surface if a MSD or a similar normal shock is present in the jet, and is caused by the slipstream (fig. 2). A vortex ring might be expected to obstruct the efficient removal of molten metal and debris from a potential cut.

The above described phenomena suggest that a cutting jet with a MSD above the workpiece is unsuitable for effective removal of material from a laser cut kerf.

The nozzle pressure above which a MSD occurs is relatively low for a circular nozzle exit of practical diameter. A non-circular exit can create a different oblique shock structure in which a MSD does not occur until high nozzle pressures.

EXPERIMENTAL METHODS AND APPARATUS

Pressure Measurements

Workpiece pressure measurements of supersonic impinging air jets are performed using a miniature piezo resistive pressure transducer behind a 0.5mm diameter pinhole in a 75mm diameter brass disk. The amplified signal from the transducer is put into the Y channel of an X-Y recorder. A second pressure transducer of the same type is used to monitor the nozzle pressure.

The disk with pressure transducer is mounted on a X-Y-Z translation stage driven by three motors, each providing an electronic position signal that can be put into the X-channel of the X-Y recorder (fig. 3a). In this fashion workpiece pressure scans along or across the jet are possible.

Alternatively, if the signal from the pressure transducer in the nozzle is put into the X-channel of the recorder, the workpiece pressure can be recorded as a function of the nozzle pressure for fixed nozzle to workpiece distance.

Flow Visualisation

A monochrome single lens schlieren flow visualisation method is used to observe the shocks in the jets. Although this method gives only qualitative results, it can be useful for inspecting jets from experimental cutting nozzles.

The Nozzles

The conical nozzle that has been investigated in this experiment is shown in fig. 3b. Early experimental nozzles had exits consisting of stacked thin (75μm) copper disks with a photo etched non-circular orifice. Although having good reproducibility, this method of making nozzle exits is complex and time consuming.

Nozzles with NC wire spark eroded exits were used to obtain the results presented here. Wire spark erosion is a relatively inexpensive and quick manufacturing process, although some detail of the orifice pattern is lost due to the finite radius of the spark wire (0.09mm). The orifice thickness can be adjusted by milling off thin layers of the nozzle tip with a diamond tool, giving a flat nozzle tip. The surface finish of the entrance of the nozzle channel cannot be adjusted and showed minor irregularities.

NOZZLE INVESTIGATIONS

Circular Nozzle Exit

Fig. 4a shows the variation of the workpiece pressure p_w as a function of nozzle pressure p_n and nozzle to workpiece distance z for a circular nozzle exit. The jet is subsonic (no shocks) for p_n<89kPa(g). Above this pressure the jet becomes supersonic and p_w is no longer monotonic. If the nozzle pressure is kept constant and z is increased from zero, the workpiece pressure decreases due

to a MSD that truncates the shock from the nozzle ((1) in fig. 4b). This MSD is caused by the presence of the workpiece and would not exist in the corresponding free jet. The range of nozzle to workpiece distances for which this normal shock exists is in this paper referred to as zone A. For increasing z the MSD gets stronger but smaller in diameter until it vanishes and regular intersection at the jet axis occurs instead ((2) in fig. 4b). At this nozzle distance the workpiece pressure rises suddenly. This region of high pressure is here referred to as zone B. If the flow after passing through the intersected shock is still supersonic, a relatively weak shock parallel and close to the surface is formed. The intersected shock can reflect on the jet boundary and cause high pressure regions similar to zone B further away from the nozzle.

Ward[7] has found a modification of the empirical Prandtl formula (Prandtl[6]) that gives the distance L from a nozzle with exit diameter D at which a zone B can be expected:

$$L = D[0.5 + 0.089\sqrt{(p_n - 90)}] \qquad (2)$$

(p_n in units of kPag)

For p_n>400kPa(g) the size of the MSD in zone A does not reduce to zero for increasing nozzle distance, but maintains a finite diameter, equal to the size of the MSD in the corresponding free jet ((3) in fig. 4b). Consequently, there is no sudden rise in workpiece pressure and zone B does not exist. Workpiece pressure variations further away are caused by reflected oblique shocks. The flow here is governed by the MSD with slipstream and a potential vortex ring. A cutting jet with a MSD can only give a high workpiece pressure close to the nozzle in zone A.

Fig. 4c shows a grease mark of an impinging jet with vortex ring from a circular exit nozzle, together with a transverse workpiece pressure scan. The grease mark was obtained by applying a small amount of thick black grease on the surface, and impinging the jet on it for a few seconds. The single streak of unremoved grease is caused by minor damage to the nozzle tip.

Cutting trials show a strong correlation between maximum cutting speed and measured workpiece pressure. The cutting speed shows a minimum for a nozzle pressure and nozzle distance for which a vortex ring can exist (fig. 4d). The axial symmetry of the converging shock from a circular nozzle exit causes Zone B to decay at relatively low nozzle pressure (due to creation of a MSD with vortex ring).

Non-Circular Nozzle Exits

A nozzle exit that is not circular can create a different initial shock structure in which a MSD can not exist until high nozzle presures are reached, resulting in a zone B with high workpiece pressure.

Fig. 5 shows the shapes of non-circular nozzle exits that have been assessed in the current experiments. Pressure distributions (i.e. workpiece pressure against nozzle pressure and nozzle to workpiece distance) are recorded from the impinging jet from each exit. Most pressure distributions have the same shape as for a circular exit i.e. zone B is present if the corresponding free jet has no MSD.

The shapes numbered 8, 14 and 32 show a zone B with high workpiece pressure for reasonable nozzle pressure, at such distances from the nozzle that an f/6 focused laser beam with its focal point in zone B will not damage the nozzle edge.

The zone B of shape numbers 1 to 7, 9 to 13, 16, 17 and 26 to 31 have an uninteresting low value of the maximum workpiece pressure, while shape numbers 15, 18 to 21, 33 and 34 show a zone B that is too far away from the nozzle. The remaining shapes (22 to 25) do not show a zone B, but a long zone of constant pressure with rapid small scale fluctuations.

Fig. 6a shows the workpiece pressure as a function of nozzle distance and fig. 6b as a function of nozzle pressure for exit shape No. 8. A 10% variation in workpiece pressure in zone B allows a tolerance in distance of 0.7mm or 60kPa in nozzle pressure (fig 6b). These tolerances are larger than those that would be reached close to the nozzle in zone A and therefore more practically useful. It should be noted, however, that a small increase in nozzle pressure or decrease in distance outside these tolerances would result in a large drop of workpiece pressure.

The high pressure zones further away occur at too large a distance for an f/6 focused laser beam. Fig. 6a is obtained from the complete pressure distribution shown in fig. 6c.

Pressure distributions have been recorded for various nozzle orifice thicknesses. Fig. 7 shows the values of nozzle pressure, distance and workpiece pressure of the optimum working point in zone B as a function of orifice thickness for three non-circular exits. A thickness (fig 3b) of 0.25-0.30mm gives high workpiece pressures at reasonable nozzle pressures and distances (table 1). Thinner orifices lack resistance against burning damage from a misaligned laser beam or reflected radiation from the cut, and may be deformed by high pressure ratios over the exit.

Table 1 - Optimum Nozzle Parameters

A 10% variation in p_w allows the given tolerances in either p_n or z.

Shape No.		8	14	32
Nozzle pressure	p_n(kPag)	6.1±0.4	6.3±0.3	8.9±0.4
Workpiece pressure	p_w(kPag)	4.7	4.5	6.3
Orifice thickness	h(mm)	0.25	0.30	0.30
Working distance	z(mm)	4.4±0.3	6.8±0.4	5.9±0.3

Fig. 8 shows the distances of the working points from table 1 as a function of the smallest radius of the exit shape. The values of z are well within the maximum distance for an f/6 focused beam.

Fig. 9a shows transverse workpiece pressure scans in the impinging jet from nozzle exit number 32. When the workpiece is in zone B the pressure shows a high maximum value at the centre of the impingement area while moving the workpiece into the low pressure region just before zone B results in a pressure distribution with decentralised peaks, indicating a vortex ring which is broken up in several 'bubbles'. This can be seen in fig. 9b. Schlieren photographs from the corresponding flows (Fig. 9c and 9d) show the simple intersection for zone B and the MSD with vortex ring in the low pressure region. Each lobe of the exit pattern can generate its own small MSD. For unequally sized lobes the corresponding small MSD's are not at a uniform distance. Jets from damaged nozzles with exit No. 32 show scattered MSD's and a significantly lower workpiece pressure in Zone B.

CONCLUSIONS

Extensive cutting trials with these non-circular nozzle shapes have yet to be performed. However, cutting trials with an experimental nozzle with an exit

very similar to No. 8 in this experiment have demonstrated that, in Zone B, the cutting speed still increases for increasing workpiece pressure for values of the latter up to 410kPa(g).

The results from this experiment suggest the following precautions:

1. Avoiding a Mach shock disk in the cutting jet, with a potential vortex ring on the workpiece surface.
2. Use of workpiece pressure and not nozzle pressure as the measured cutting parameter.
3. Use of a nozzle with suitable non-circular exit e.g. No. 8, 14 or 32 in this experiment.
4. Working in Zone B for high workpiece pressure at a damage-resistant nozzle distance from the work, with large tolerances in nozzle pressure and position.
5. Use of a pressure probe to locate Zone B.
6. Tight quality control of the nozzle exit.
7. Taking care to protect nozzles from damage.

ACKNOWLEDGEMENT

This work has been sponsored by the Reprocessing Development Working Party of the Northern Division of the United Kingdom Atomic Energy Authority.

REFERENCES

1. Donaldson, C. Dup. and Snedeker, R.S., "A study of free jet impingement. Part 1. Mean properties of free and impinging jets". J. Fluid Mech., Vol. 45, Part 2, pp281-319 (1971).
2. Ginzburg, I.P., Semiletenko, B.G., Uskov, V.N., "Experimental study of underexpanded jets impinging normally on a plane baffle". Fluid Mech. Soviet Research, Vol. 4, No. 3, pp93-105 (1975).
3. Gubanova, O.I., Lunev, V.V., Plastinina, L.N., "The central breakaway zone with interaction between a supersonic underexpanded jet and a barrier", Fluid Dyn., Vol. 6, pp298-301 (March 1973).
4. Kalghatgi, G.T. and Hunt, B.L., "The occurrence of stagnation bubbles in supersonic jet impingement flows", Aeronautical Quarterly, Aug 1976, pp169-185.
5. Von Mises, R., "Mathematical theory of compressible fluid flow", Academic Press, New York, 1958.
6. Prandtl, L., "The essentials of fluid dynamics", Blackie & Son, Glasgow, 1952.
7. Ward, B.A., "Supersonic characteristics of nozzles used with lasers for cutting", Paper presented to the International Congress of the Applications of Lasers and Electro-Optics, Boston, MA, USA, 12-15th Nov 1984.

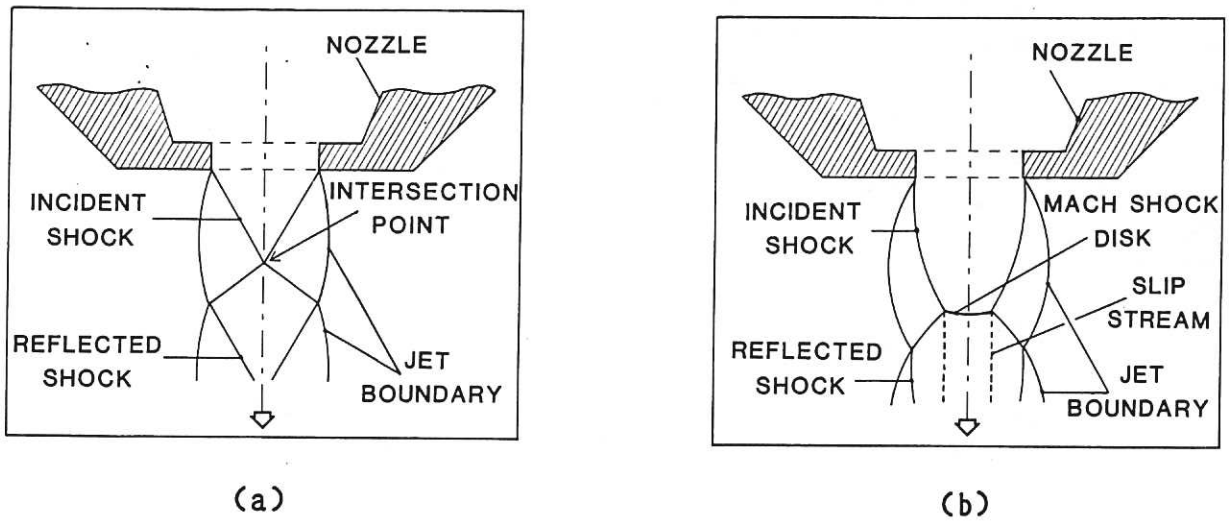

Fig. 1 Shock structure in a supersonic jet. (a) Regular intersection. (b) Mach reflection with Mach shock disk.

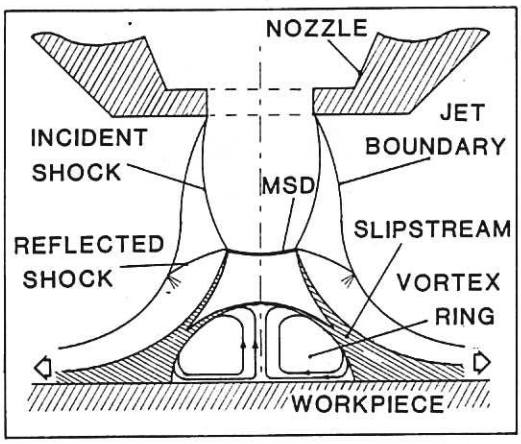

Fig. 2 Vortex ring on workpiece surface.

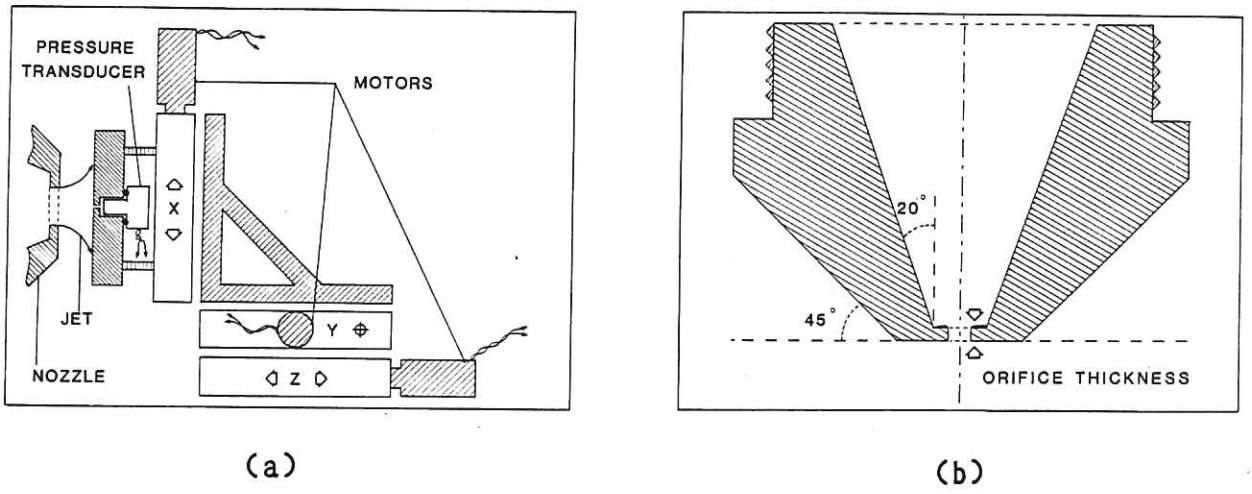

Fig. 3 (a) Pressure scanning apparatus. (b) Laser cutting nozzle.

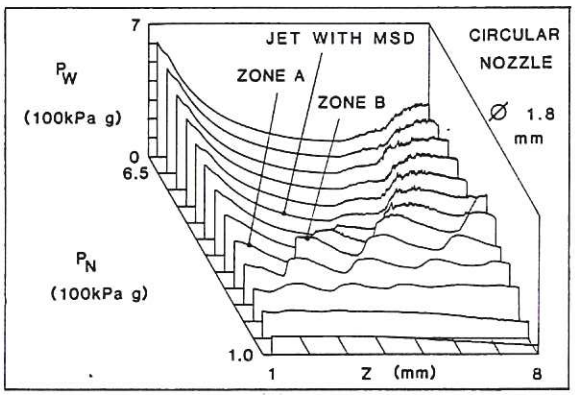

(a)

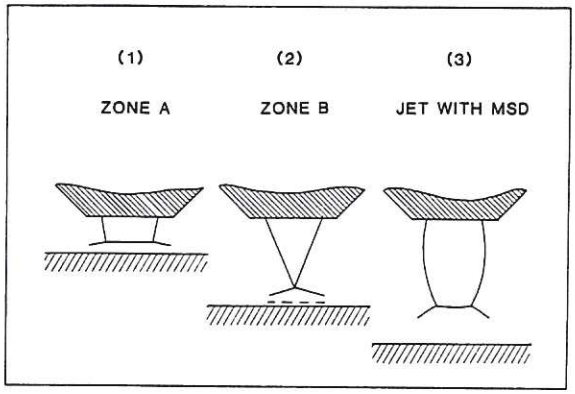

(b)

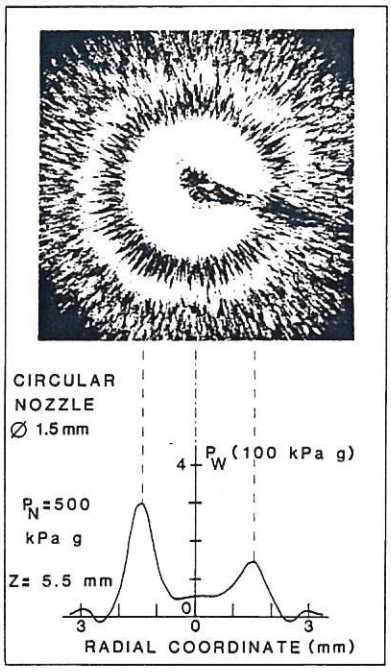

(c)

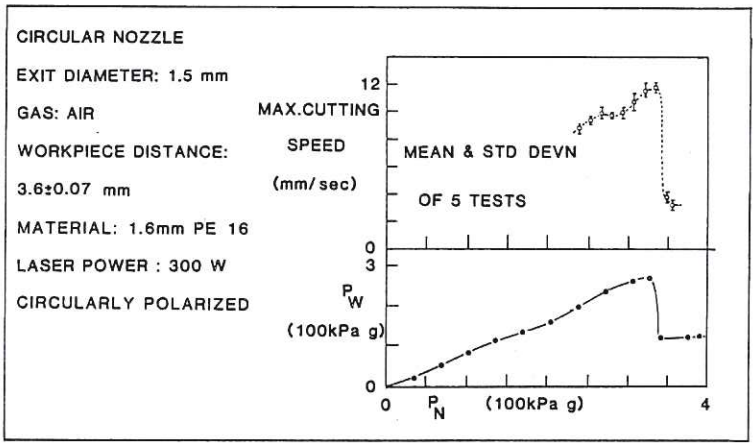

(d)

Fig. 4 (a) Workpiece pressure distribution of an impinging jet from a circular nozzle.
(b) Shock structure in impinging jets.
(c) Grease mark from flow with vortex ring.
(d) Cutting trials.

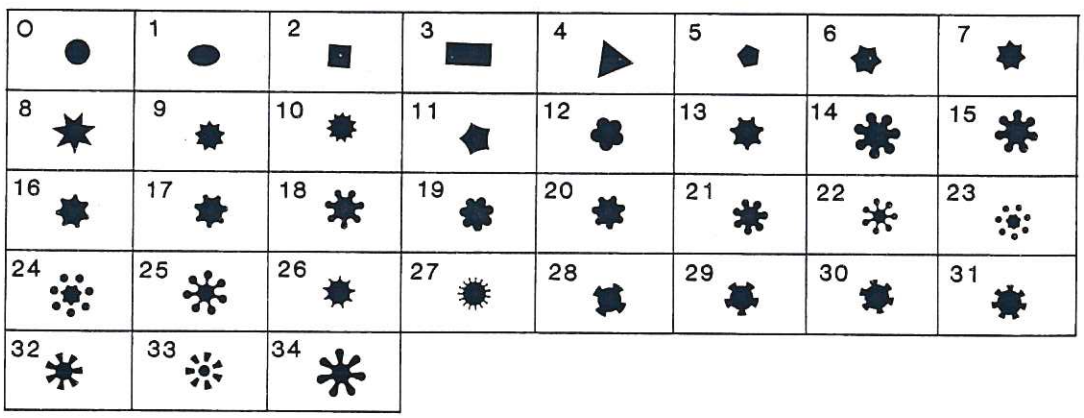

Fig. 5 Non-circular exits (approximately 2 x actual size).

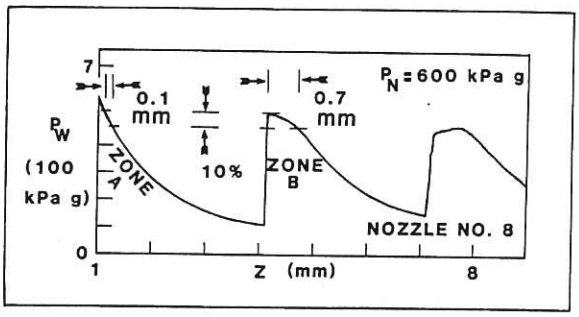

(a)

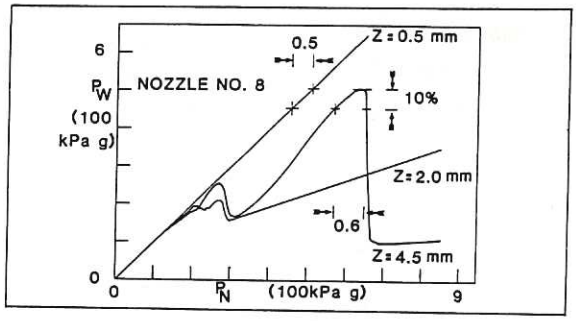

(b)

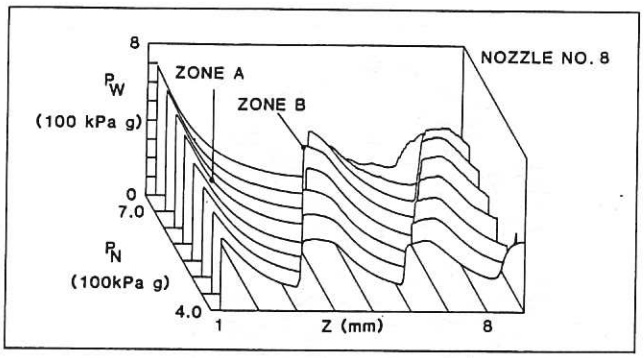

(c)

Fig. 6.
(a) Variation of workpiece pressure with nozzle distance for nozzle no. 8.
(b) Dependence of workpiece pressure on nozzle pressure.
(c) Workpiece pressure distribution.

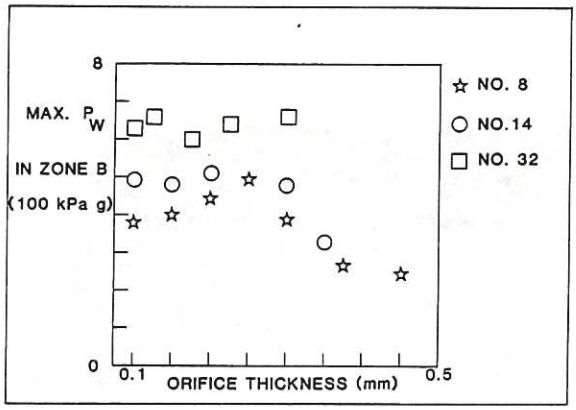

(a)

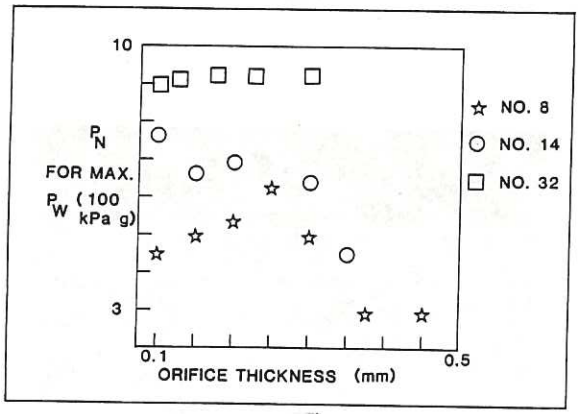

(b)

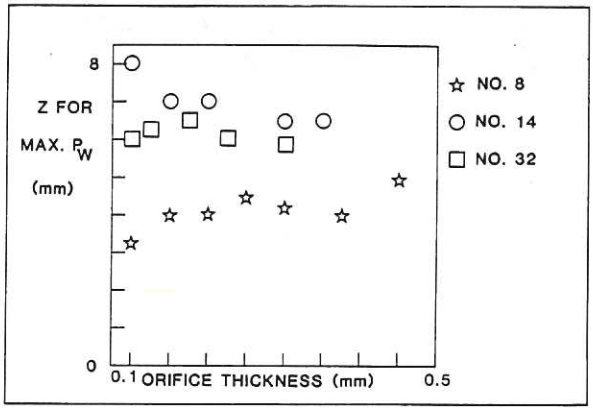

(c)

Fig. 7.
(a, b & c) Dependence of the optimum working point in zone B on the orifice thickness (Fig. 3.(b)).

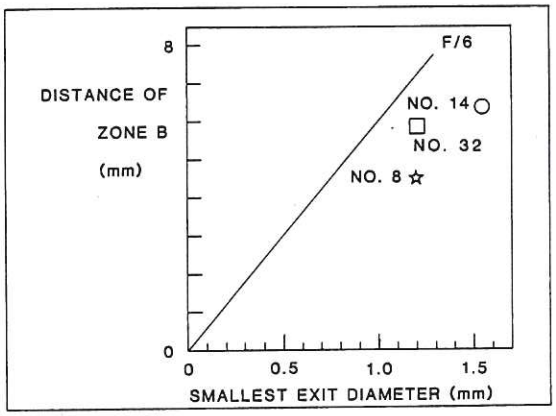

Fig. 8 Location of zone B as a function of smallest diameter in non-circular exit.

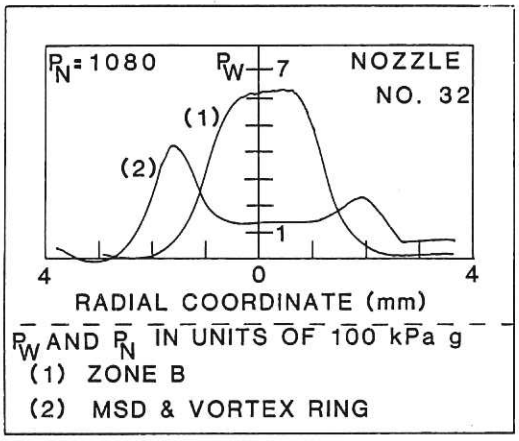

(a)

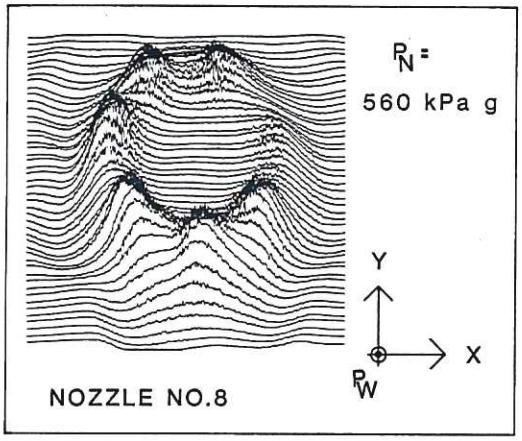

(b)

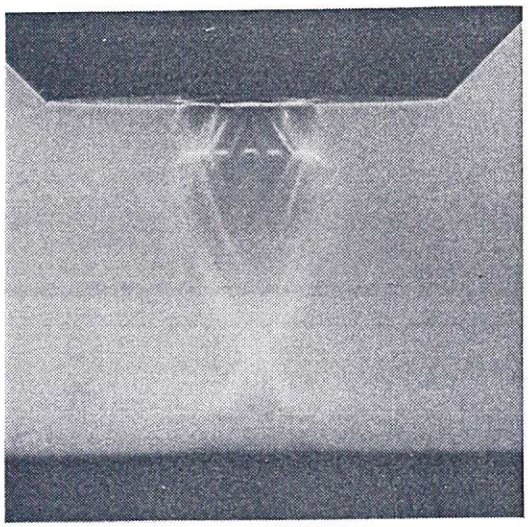

(c)

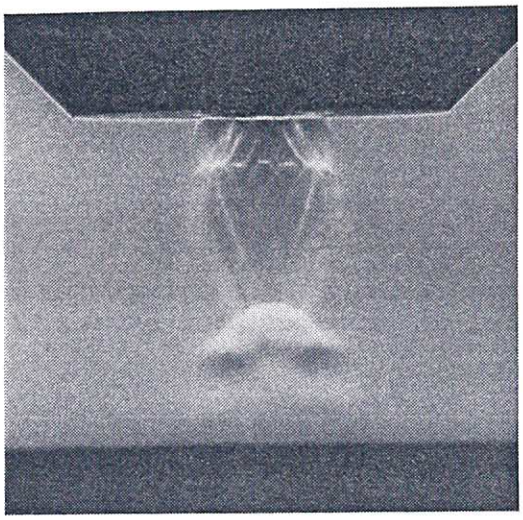

(d)

Fig. 9 (a) Radial scans across jet axis (b) Radial pressure profile of impinging jet with vortex ring. (c&d) Schlieren photographs of the jet in zone B (9c) and with MSD and vortex ring (9d), corresponding to Fig. 9a.

F-Hollman
E6 113